Desalination and Water Treatment
www.deswater.com

doi: 10.5004/dwt.2018.23129

135 (2018) 133–140
December

Mechanism of red mud combined with steel slag conditioning for sewage sludge dewatering

He Li[a], Min Zhou[a], Yi Han[b,*], Bingchen Shi[a], Qiao Xiong[a], Haobo Hou[a,*]

[a]*School of Resource and Environment Science, Wuhan University, Wuhan 430072, China, email: whuheli@163.com (H. Li), zhoumin@whu.edu.cn (M. Zhou), 738890392@qq.com (B. Shi), 396151758@qq.com (Q. Xiong), 1142820672@qq.com (H. Hou),*
[b]*School of Resource and Environment, Anqing Normal University, Anqing, 246011, China, email: yihan@whu.edu.cn*

Received 27 March 2018; Accepted 13 September 2018

ABSTRACT

Red mud (RM), which is a byproduct of alumina refining, is typically stored in landfills. This study investigated the capability of RM combined with steel slag to improve sludge dewatering performance. When the RM dosage was 20 mg/g, the HCl/RM ratio was 0.6, and the steel slag dosage was 3 mg/g DS, RM combined with steel slag exhibited a good conditioning capability as the pH of the filtrate approached neutrality. This result indicates that the coagulation of RM by Fe^{3+} and Al^{3+} is critical in sludge conditioning and that the steel slag acts as a neutralizer and a skeleton builder. Thus, four mechanisms of RM and steel slag were proposed for sewage sludge conditioning. First, Fe^{3+} and Al^{3+} generated from RM acted as coagulants that agglomerated small sludge particles into large dense particles with low bound water. Second, extracellular polymeric substances (EPS) were degraded into proteins by RM. Third, the released proteins were destroyed by the steel slag. Last, the bound water was converted into free water due to EPS degradation.

Keywords: Red mud; Steel slag; Sludge dewatering; Extracellular polymeric substance; Particle size distribution

1. Introduction

Sewage sludge is a byproduct of wastewater treatment plants (WWTPs) [1]. The treatment and disposal of sewage sludge are limited by its poor dewatering efficiency [2]. Sludge is difficult to dewater because of the bound water, including interstitial water, surface/vicinal water, and intracellular water. Thus, sludge conditioning is typically applied as a pretreatment prior to dewatering [3–5].

Researchers have developed many conditioning techniques, such as chemical conditioning [6], thermal treatment [7], ultrasonication [8], and electrode watering [9]. Among these methods, chemical conditioning can easily and effectively destroy the polymeric matrix and facilitate the release of extracellular polymeric substances (EPS) and bound water in sludge flocs [10]. Conventional chemical additives include aluminum sulfate, ferric chloride, polyelectrolyte, enzymes, surfactants, etc. [11]. Xin et al. used calcium carbonate ($12CaO{\cdot}7Al_2O_3$) and sulfoaluminate ($Ca_3Al_6O_{12}{\cdot}CaSO_4$) synthetic binders to perform deep dewatering of excess sludge before landfilling [12]. Li et al. found that CaO can improve sludge dewatering performance as the dissolution of CaO releases heat. Moreover, the pH is increased to 8.85 ± 0.06, which destroys the flocculation structure and improves the compressibility of the sludge [13].

Red mud (RM) is a solid waste generated in alumina refining from bauxite [14]. Approximately 70 million tons of RM is generated per year worldwide, causing serious environmental problems [15,16]. Therefore, effective utilization methods for RM must be urgently developed [17]. RM has been used as a construction or ceramic material (bricks, tiles, and cement) [18], an adsorbent [19], soil amendment [20], and metal recovery [21]. Nonetheless, the recycling and reuse of RM remain inadequate, and limited attention has been directed toward sludge conditioning by RM. Zhang et al. utilized sewage sludge conditioned by RM as an alternative skeleton builder [22].

Steel slag is a byproduct of the conversion of iron into steel, and it exhibits different properties depending on the raw materials and processes used [23]. Fifty million tons of

*Corresponding author.

1944-3994 / 1944-3986

steel slag are produced every year as residues worldwide [24]. The utilization of this byproduct is relatively low in China. Studies on the recycling and utilization of steel slag have been recently conducted in different fields [25–28]. Steel slag has been applied in the construction and stabilization of dams, dikes, embankments, road buildings, and agriculture [29].

In this study, RM was modified by HCl combined steel slag to improve sludge dewaterability. The schematic of this process is shown in Fig. 1. This study aimed to (1) demonstrate the feasibility of using RM as a conditioner by evaluating the dewaterability of the conditioned sludge and the pH of the filtrate; (2) optimize the dosages of RM and steel slag and the HCl/RM ratio; (3) explore the mechanisms of the composite conditioner in terms of the EPS, bound water content, and microstructure of the sludge; and (4) preliminarily evaluate the cost of using the optimal dosages of RM and steel slag for sewage sludge dewatering.

2. Methods

2.1. Materials

The raw sewage sludge (RS) was composed of a mixture of primary and secondary sludge from Sanjintan WWTP, Wuhan, China. This municipal WWTP has a capacity of 3 × 10^5 m^3/d. RS samples were collected in polypropylene containers and stored at 4°C in a refrigerator for at most 4 days [30,31]. The main characteristics of the RS are listed in Table 1.

The RM used was a residue of bauxite that was treated using the Bayer process. The RM originated from the Shan Dong branch of the Aluminum Corporation of China. The pH was 12.7. The chemical and mineral compositions of RM were analyzed by X-ray fluorescence and X-ray diffraction, as shown in Table 1 and Fig. 2. The main chemical components of the RM were Fe_2O_3, Al_2O_3, and SiO_2. The mineralogical phases of the RM were hematite, gibbsite, cancrisilite, and dickite.

The steel slag was obtained from Wuhan Iron and Steel Corporation, China. It was crushed to less than 80 μm by grinding in a laboratory ball mill for 30 min. The main chemical compositions are listed in Table 2. After the steel slag was sifted through the screen, many fine but uneven particles appeared. The surface was irregularly shaped, and the outer particle outline was an irregular polyhedron. The microstructure of steel slag is shown in Fig. 3.

2.2. Sludge conditioning and dewatering

Refrigerated sludge was recovered to the interior temperature under natural conditions, diluted with deionized water to 95%, and rapidly stirred for 1 h to evenly mix the sludge and the water. After mixing, the sludge was screened through a 1.2 mm sieve to remove the large particles. 500 mL handle sludge samples were placed on the experimental device and then conditioned with the following procedure: addition of RM → 270 rpm stirring for 5 min → addition of HCl → 270 rpm stirring for 5 min → addition of steel slag → 200 rpm stirring for 5 min.

2.3. EPS extraction and analysis

The EPS of the sludge can be divided into three groups: supernatant layer EPS (S-EPS), loosely bound EPS (LB-EPS), and tightly bound EPS (TB-EPS) [32,33]. EPS are critical factors that influence sludge dewaterability [34]. The LB-EPS

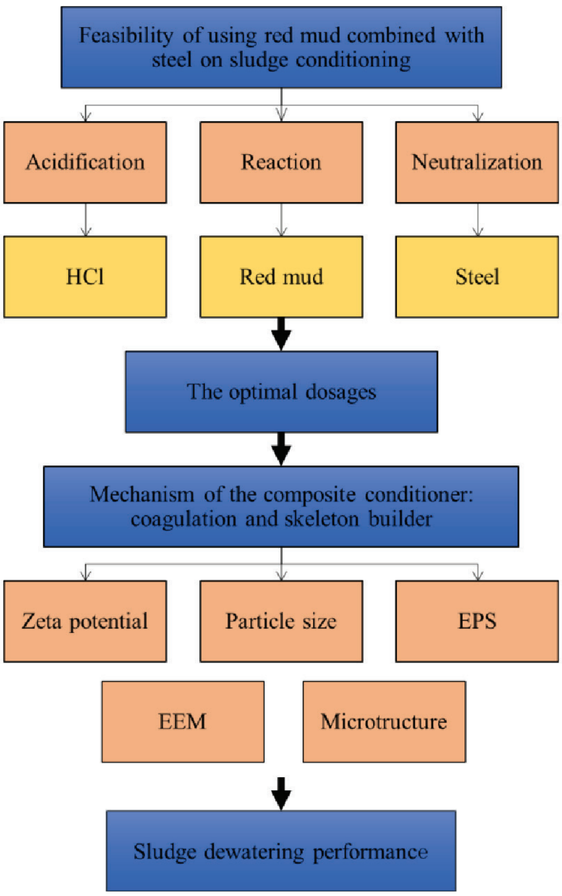

Fig. 1. Schematic of the study.

Table 1
Basic characteristics of the raw sludge

Para-meters	Moisture (%)	pH	Organic content (%)	CST(s)	SRF (×10^{13} m/kg)
Raw sludge	95.02 ± 1.8	7.18 ± 0.14	39.10 ± 0.31	149.1 ± 6.8	2.0 ± 0.9

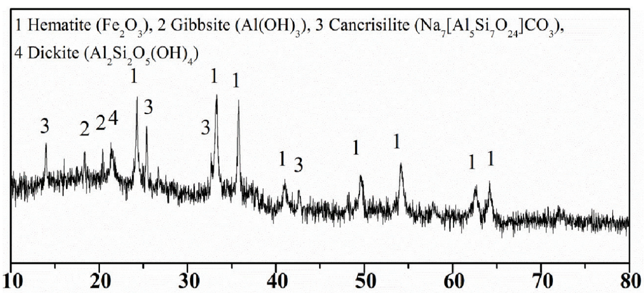

Fig. 2. Mineral composition of RM.

Table 2
Main inorganic chemical compositions of steel slag (wt %)

Constituents	MgO	Al_2O_3	SiO_2	P_2O_5	SO_3	CaO	TiO_2	MnO	Fe_2O_3	LOI[a]
RM	–	20.26	12.84	0.13	0.59	0.86	7.35	0.02	33.39	12.28
Steel slag	5.28	3.19	18.67	1.26	0.53	40.77	0.39	1.37	12.01	

[a]LOI = loss of ignition.

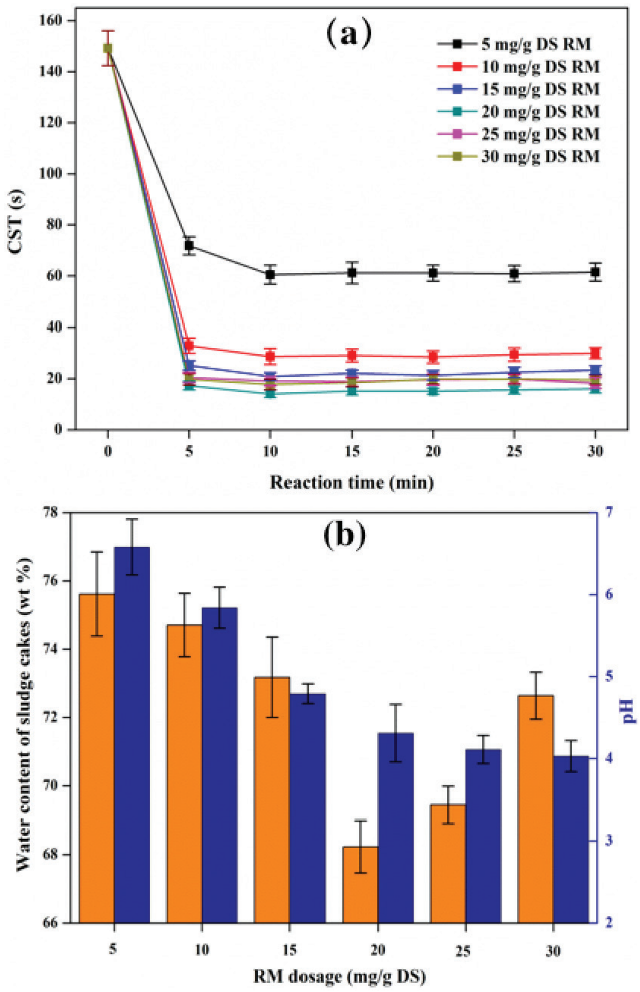

Fig. 3. Effects of the RM dosage on conditioning sludge: (a) CST, and (b) Wc.

and TB-EPS were extracted from the sludge by using a modified heat extraction method according to the procedures of Li et al. [35]. The particulates in the two EPS fractions were removed using polytetrafluoroethylene membranes with a pore size of 0.45 µm prior to organic analysis [36].

2.4. 3D excitation-emission matrix (EEM)

The EEM spectra comprise a series of emission spectra over a range of excitation wavelengths that can be used to identify the fluorescent compounds in complex mixtures. The peak locations, peak intensities, and ratios of different peaks in the EEM spectra of the EPS samples were not substantially influenced by ionic strength. The 3D-EEM spectra were obtained by a Hitachi F-4500 fluorescence spectrophotometer with an excitation range of 200–400 nm at 5 nm sampling intervals and an emission range of 220–550 nm at 5 nm sampling intervals. The spectra were obtained at a scan rate of 12,000 nm/min with excitation and emission slit bandwidths of 3 nm. Each scan exhibited 67 emissions and 41 excitation wavelengths. Origin 8.0 (OriginLab Inc., USA) was employed to process the EEM data [37].

2.5. Analysis of other items

Sludge dewatering performance was evaluated on the basis of capillary suction time (CST), specific resistance to filtration (SRF), and water content of sludge cakes (WC). The CST was measured using a 304 M CST instrument (Triton, UK). The SRF was measured using a multi-coupled measuring device. The sludge cakes were dried at 105°C for 24 h to determine their water content. The zeta potential was tested using a Malvern Zetasizer Nano ZS (Malvern Instruments Ltd., UK) by collecting the supernatant of the sludge after centrifugation at 4500 rpm for 5 min before the supernatant was collected and mixed with the sludge at a ratio of 9:1. Particle size distribution was determined with a Mastersizer 2000 laser particle-size analyzer (Malvern, UK) at a stirring rate of 1000 rpm after the sludge was dispersed in an aqueous solution. The microstructural characteristics of the raw and conditioned sludge samples were investigated through scanning electron microscopy (Quanta 200, FEI).

3. Results and discussion

3.1. Effect of RM dosage

The effect of RM dosage on sludge dewatering performance was examined at six different dosages (5, 10, 15, 20, 25, and 30 mg/g DS) with a HCl (mL)/RM (g) ratio of 0.8. The corresponding CST, W_C, and pH values at different RM dosages are provided in Fig. 3. As shown, nearly all possible reductions in CST occurred within 5 min, but the reduction in CST became negligible after 10 min and even presented a side effect over time. The CST obviously decreased when the RM dosage was increased from 5 mg/g DS to 15 mg/g DS, and the CST reduction efficiency reduced when the RM dosage exceeded 20 mg/g DS. The change rule in Wc was similar to that in CST. As the RM dosage was increased, the minimum Wc was obtained at 20 mg/g DS. Therefore, the optimal RM dosage was 20 mg/g DS. The pH of the supernatant gradually decreased with increasing RM dosage, and the pH was 4.31 when the dosage was 20 mg/g. RM is a source of Fe^{3+} and Al^{3+}. As such, increasing of RM dosage enhanced sludge dewatering. RM is highly alkaline and can be neutralized by soaking with HCl. However, excessive HCl would reduce the supernatant pH of the sludge and result in strong acidity, which does not satisfy the discharge standard.

3.2. Effect of HCl/RM ratio

The addition ratio of HCl and RM directly affects the leaching of Fe^{3+} and Al^{3+} as well as the pH of the sludge and the supernatant. Therefore, the effects of the HCl/RM ratio on sludge dewatering, W_C, and supernatant pH were investigated. On the basis of the preceding experimental results, the RM dosage was fixed at 20 mg/g DS. The sludge dewatering performance was significantly improved when the HCl/RM ratio was increased from 0.2 to 0.6, and the reduction rate in CST was insignificant when the HCl/RM ratio was greater than 0.6. As shown in Fig. 4, the water content of the mud cake initially decreased gradually and then increased gradually when the ratio was more than 0.8. As the dosing ratio was increased, the pH of the sludge supernatant decreased gradually. When the ratio was 0.6 or lower, the supernatant was weakly acidic, but the pH was reduced to less than 5 when the ratio was increased. Therefore, the HCl/RM ratio of 0.6 was considered the most suitabl e for improving the dewatering performance of the sludge. The colloidal structure of Fe^{3+} could be destroyed by excessive HCl and weaken its flocculation effect. However, an excessive acidity would release the substance from EPS into liquid phase. Most of the dissolved EPS were water soluble and therefore unconducive for water removal.

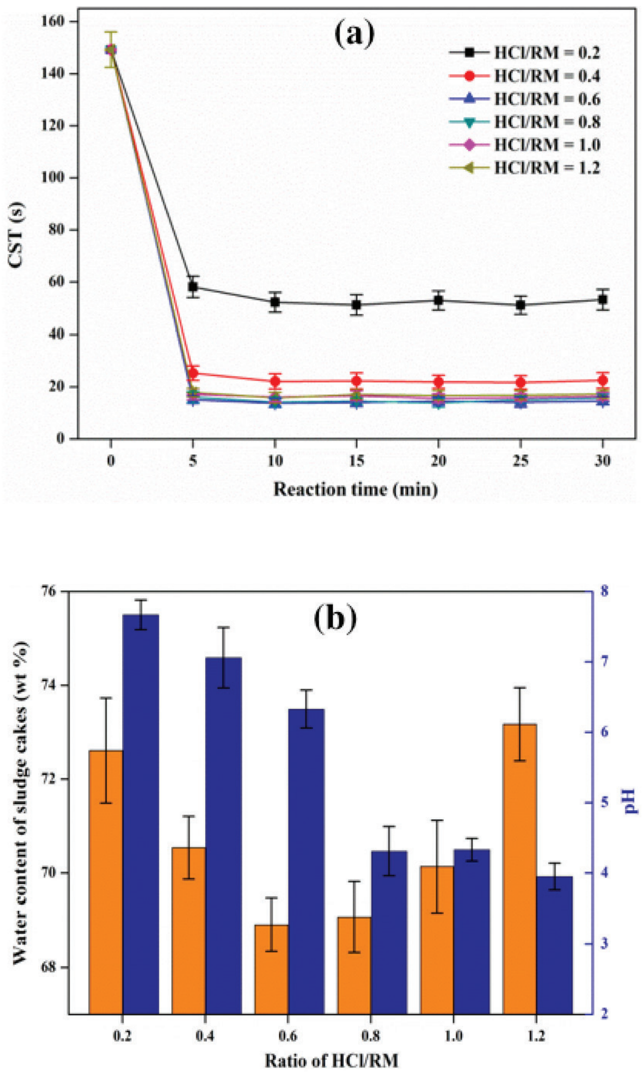

Fig. 4. Effects of HCl/RM ratio on conditioning sludge: (a) CST, and (b) Wc.

3.3. Effect of steel slag dosage

On the basis of the experimental results in Sections 3.1 and 3.2, the RM dosage of 20 mg/g DS and the HCl/RM ratio of 0.6 were set as fixed experimental parameters. The influence of the dosage of the steel slag on improving the dewatering performance of sludge was examined. The variations in sludge dewatering performance in terms of CST, SRF, and W_C are presented in Fig. 5. As shown, the addition of steel slag further improved sludge dewatering performance. As the steel slag dosage was increased, the CST and SRF values of the sludge displayed a downward trend. The results of CST showed that the dewatering performance significantly improved when the amount of steel slag was increased from 1 mg/g DS to 3 mg/g DS. When the steel slag dosage was greater than 3 mg/g DS, the decrease in CST became insignificant. This phenomenon may be related to the self-measurement error of the CST instrument because the CST value was less than 10 s, which was close to the test value of pure water. SRF results showed that the SRF decreased continuously with increasing dosage. When the dosage was more than 3 mg/g DS, the rate of SRF decrease slowed down. The change tendency of the Wc was similar to that of the SRF. When the steel slag dosage was 3 mg/g DS, the water content of the mud cake significantly reduced, although the decrease eventually became insignificant. The supernatant pH increased gradually with increasing steel slag dosage. The alkalinity of the steel slag can neutralize excessive HCl, thereby improving the supernatant pH, and an excessive addition of the supernatant would make the supernatant alkaline. Therefore, in consideration of these findings and the actual cost, a steel slag dosage of 3 mg/g DS was selected as the best choice.

3.4. Possible mechanisms of improved sludge dewaterability

3.4.1. Effect of zeta potential on dewaterability

Extracellular polymers are important components in the bioflocculation, settling, and dewatering of activated sludge [11,38]. The zeta potential is significantly related to extracellular polymers because a decrease in the sludge negative charge could reduce the repulsion forces and enhance the compaction of sludge flocs [11]. Zhang et al. demonstrated a strong correlation between SRF and zeta potential (R^2 = 0.99, p < 0.01) [39], suggesting that the zeta potential could partly reflect sludge dewatering performance. The effects of RM and steel slag on the zeta potential of the sludge supernatant are depicted in Fig. 6.

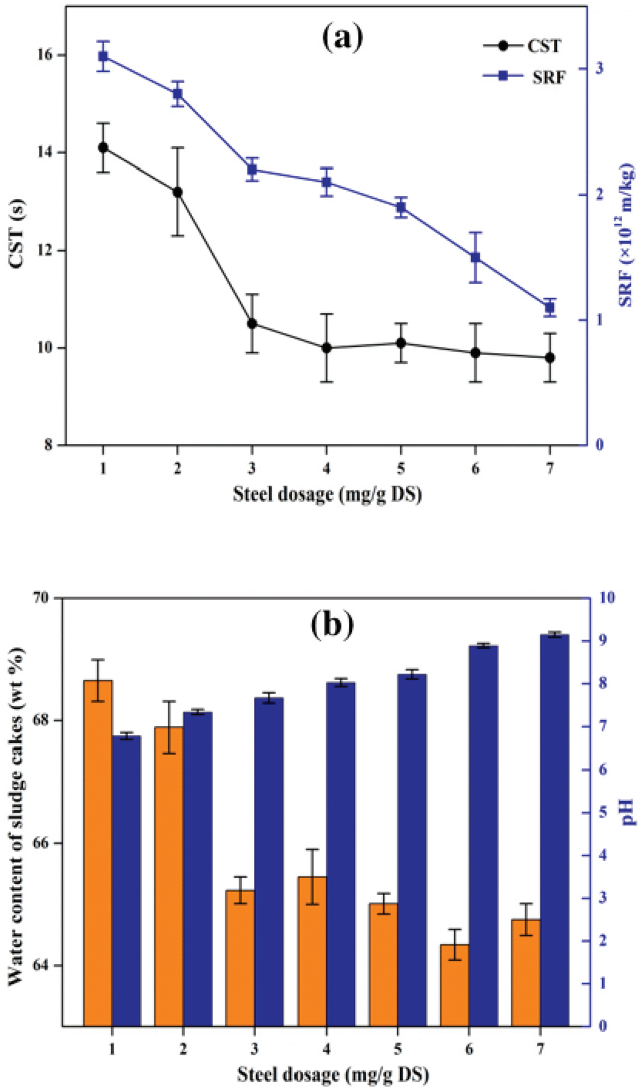

Fig. 5. Effects of the steel slag dosage on conditioning sludge (a) CST and SRF, and (b) Wc.

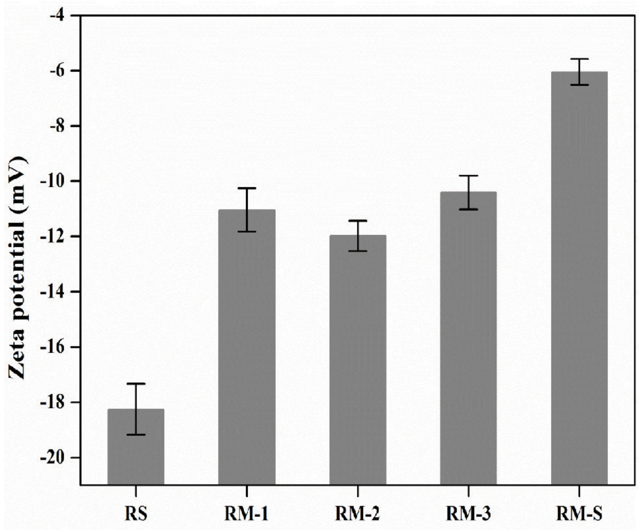

Fig. 6. Changes of Zeta potential: RS: raw mud, RM-1: 20% RM and HCl/RM = 0.6, RM-2: 20% RM and HCl/RM = 0.8, RM-3: 30% RM and HCl/RM = 0.8, and RM-S: 20% RM and HCl/RM = 0.6 and 5% steel slag.)

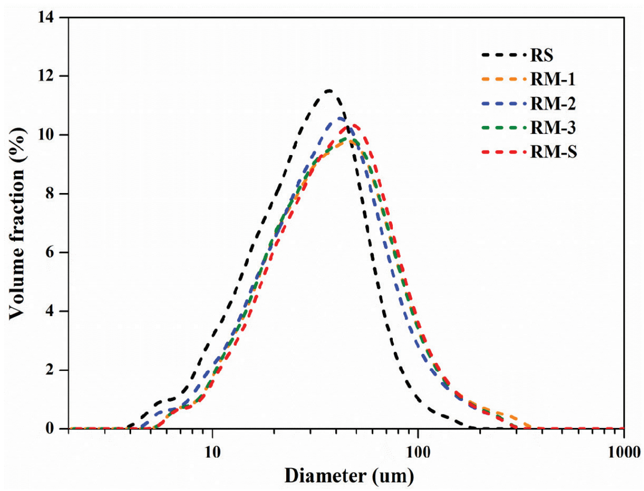

Fig. 7. Changes of particle size distribution between raw and conditioned sludge.

The surfaces of the RS were originally negatively charged with a zeta potential of −18.3 ± 0.9 mV. When 20 mg/g DS RM was added, the zeta potential decreased to −11.1 ± 0.8 mV. The zeta potential did not significantly change when the dosage of HCl or RM was increased. In the RM-2 experimental group, the zeta potential obtained by increasing the HCl ratio was higher than that in the RM-1 experimental group. When 3 mg/g steel slag was added continuously, the zeta potential decreased significantly to −6.1 ± 0.5 mV DS.

3.4.2. Effect of particle size distribution on dewaterability

The variations in particle size distribution of the sludge flocs are presented in Fig. 7. The particle size distributions of the sludge were markedly affected by RM possibly because of the flocculation of Fe^{3+} and Al^{3+} from RM. The coagulants of Fe^{3+} and Al^{3+} salts could neutralize the surface charge of the particles, thereby destabilizing the sludge particles. The sludge particles rapidly aggregated into large flocs. Then, the sludge flocs densified because of the double electric layer compression [40]. The particle size of the sludge pretreated by RM with a high HCl/RM ratio was smaller than that of the sludge conditioned by RM with a normal HCl/RM ratio. The possible reason is that the EPS structures were degraded, and the dense sludge flocs were broken into smaller particles by the superfluous acid. As the RM dosage was increased, the particle size of the sludge did not increase significantly, which was consistent with the dewatering experimental results. The addition of steel slag slightly increased the particle size distribution possibly due to the reduction of the zeta potential and the accumulation of sludge particles.

3.4.3. Effect of EPS on dewaterability

As shown in Fig. 8, proteins and polysaccharides were mainly distributed in S-EPS and T-EPS. The content of T-EPS was obviously greater than those of S-EPS and L-EPS. The addition of RM significantly increased the content of S-EPS, of which the main component was protein. This finding indicated that the addition of RM released part of the EPS that is related to the oxidation of Fe^{3+} and the action of HCl. The increase in the S-EPS increased the raise of zeta potential, which is consistent with the zeta potential analysis. In addition, S-EPS content increased as the amount of RM was increased, but excessive S-EPS was unconducive for sludge water removal, which was consistent with the results for CST and Wc. When steel slag was continuously added, the S-EPS content reduced and the protein content decreased significantly, which promoted sludge dewatering performance. These results coincided well with those of Zhen et al. [41], who showed that sludge dewaterability is highly related to soluble EPS, i.e., a large amount of soluble EPS would lead to a poor sludge dewatering performance. The results were also consistent with those of Liu et al. [42], who observed a close relationship between the protein-like substances of EPS and the filtration resistance of the membrane in membrane bioreactors.

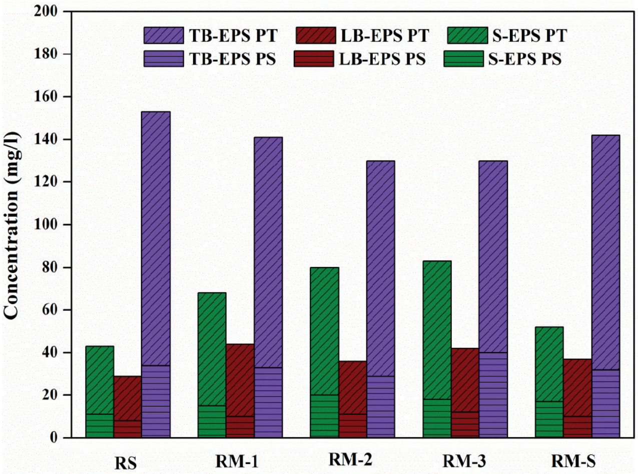

Fig. 8. Changes of EPS between raw and conditioned sludge.

Therefore, RM and steel slag can improve sludge dewatering performance. The RM releases part of the EPS, and some of the bound water is released. However, excessive EPS is unconducive for water removal. The neutralization and flocculation of Fe^{3+} and Al^{3+} reduced the zeta potential, increased the particle size, and improved the dewatering performance of the sludge. After the steel slag was added, the released protein was destroyed, and the zeta potential was further reduced, thereby improving sludge dewatering performance.

3.4.4. EEM fluorescence analysis

3D-EEM fluorescence spectroscopy is a rapid and sensitive technique for determining the fluorescence compounds in EPS and exploring the possible mechanisms of improved sludge dewaterability. As shown in Fig. 9, the main peak, which is located at the excitation/emission wavelengths (Ex/Em) of 370–390/440–470 nm (Peak A) in the EEM spectra, can be identified from the fluorescence spectra of the EPS in the control groups. Peak A was a humic acid-like organics [43]. Three other peaks were identified at the excitation/emission (Ex/Em) of 340–350/435–445 (Peak B), 280/350–360 (Peak C), and 245/450 nm (Peak D). Peak B was associated with visible humic acid-like fluorescence. Similar fluorescence signals were also reported for naturally dissolved organic matters and extracellular substances of waste-activated sludge [44–46]. Peak C, which was located at the Ex/Em of 280/350–360 nm, was a tryptophan protein-like substance, and Peak D represented fulvic acid-like substances.

The fluorescence peaks of raw mud were mainly peaks A and B. After the addition of RM, new fluorescence peaks, mainly peaks B, C, and D, appeared. Moreover, the fluorescence intensity of humic acid increased, indicating that the structures of the EPS were destroyed and that some of the EPS dissolved into S-EPS. This finding is consistent with the preceding EPS determination results. The S-EPS content, of which the main component was

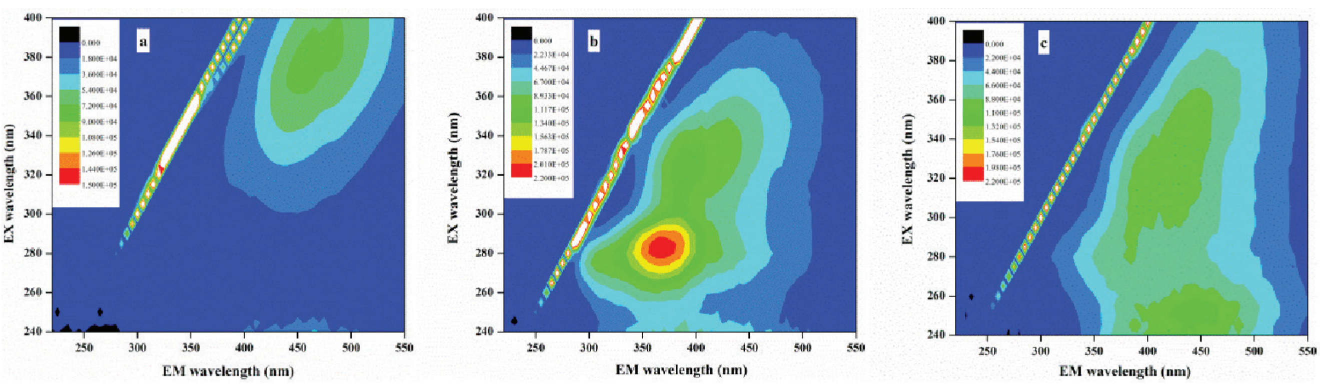

Fig. 9. EEM fluorescence spectra of the soluble EPS fractions: (a) before conditioning, (b) after treatment by RM, and (c) RM combined with Steel slag.

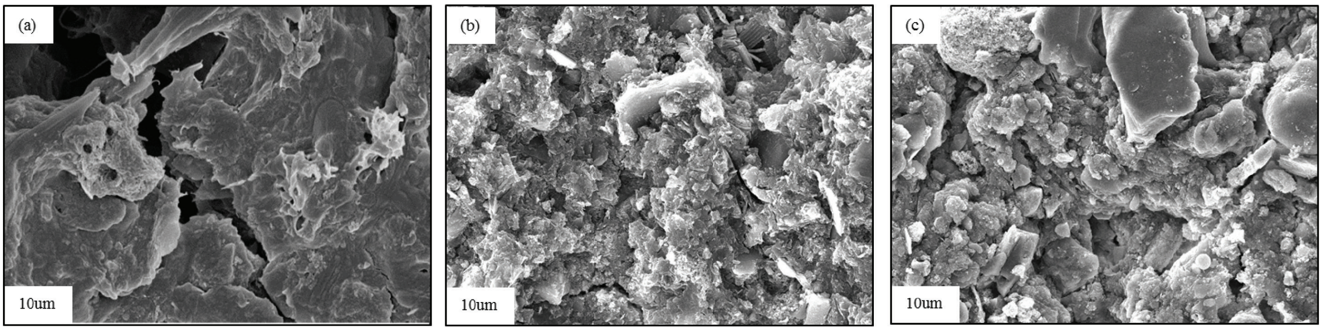

Fig. 10. SEM images: (a) raw sludge, (b) conditioned by RM, and (c)conditioned by RM+ Steel slag.

protein, increased significantly. An increase in the S-EPS generally leads to an increased surface charge and a poor dehydration performance. Therefore, the reduction of the zeta potential of the sludge after RM conditioning was mainly due to the neutralization of Fe^{3+} and Al^{3+}. The zeta potential was reduced, the particle size of the sludge was increased, and the sludge dewatering performance was improved.

After the addition of steel slag, the fluorescence intensities of peaks B, C, and D decreased, indicating that protein-like substances were destroyed, and that the existence of protein-like substances inhibited the sludge dewatering performance. The S-EPS were degraded by the addition of steel slag, and the dewatering performance of sludge was improved, which was consistent with the experimental results. The S-EPS content decreased with the addition of steel slag, and the protein content decreased significantly. The decrease in S-EPS content reduced the surface charge of the flocs, which could explain why the zeta potential of the sludge after the addition of steel slag was lower than that of the sludge added with RM.

3.4.5. Microstructure

As shown in Fig. 10, the microstructure of the RS appeared dense, indicating poor water permeability and poor dewaterability. In comparison, the conditioned sludge showed obvious changes in the structure. The original compact layered structure was destroyed, and small particles were formed. The porosity increased significantly, which was beneficial to the water circulation. The addition of steel slag resulted in the formation of small particles into large particles and the emergence of irregular blocky structures, which acted as skeleton structures in extrusion dehydration and promoted sludge dewaterability.

4. Conclusions

1. The optimal dosages of the composite conditioner were 20 mg/g DS of RM and 3 mg/g DS of steel slag. The HCl/RM ratio was 0.6. RM conditioning combined with steel slag markedly enhanced sludge dewaterability as the pH of the filtrate approached neutrality, and the steel slag acted as a skeleton builder.
2. The EPS were degraded into proteins by RM, and the released proteins were destroyed by the steel slag. The bound water was converted into free water due to the degradation of EPS. The increase in particle size and the decrease in surface charge effectively improved dewatering performance.
3. The conditioned sludge displayed a porous structure and a coagulation phenomenon. The results of this investigation suggest that RM conditioning combined with steel slag is a promising candidate for improving sludge dewaterability.

Acknowledgments

This work was financially supported by the major scientific and technological innovation subject in the Hubei province, China (No. 2016ACA162).

References

[1] R.P. Singh, M. Agrawal, Potential benefits and risks of land application of sewage sludge, Waste Manage., 28 (2008) 347–358.
[2] F.Y. García Becerra, E.J. Acosta, D.G. Allen, Alkaline extraction of wastewater activated sludge biosolids, Bioresour. Technol., 101 (2010) 6972–6980.
[3] J. Vaxelaire, P. Cézac, Moisture distribution in activated sludges: a review, Water Res., 38 (2004) 2215–2230.
[4] C.C. Wu, C. Huang, D.J. Lee, Bound water content and water binding strength on sludge flocs, Water Res., 32 (1998) 900–904.
[5] M. Huo, G. Zheng, L. Zhou, Enhancement of the dewaterability of sludge during bioleaching mainly controlled by microbial quantity change and the decrease of slime extracellular polymeric substances content, Bioresour. Technol., 168 (2014) 190.
[6] M.C. Lu, C.J. Lin, C.H. Liao, R.Y. Huang, W.P. Ting, Dewatering of activated sludge by Fenton's reagent, Adv. Environ. Res., 7 (2003) 667–670.
[7] M. Ruiz-Hernando, G. Martinez-Elorza, J. Labanda, J. Llorens, Dewaterability of sewage sludge by ultrasonic, thermal and chemical treatments, Chem. Eng. J., 230 (2013) 102–110.
[8] L. Huan, J. Yiying, R.B. Mahar, W. Zhiyu, N. Yongfeng, Effects of ultrasonic disintegration on sludge microbial activity and dewaterability, J. Hazard. Mater., 161 (2009) 1421–1426.
[9] H. Yuan, N. Zhu, F. Song, Dewaterability characteristics of sludge conditioned with surfactants pretreatment by electrolysis, Bioresour. Technol., 102 (2011) 2308.
[10] G.P. Sheng, H.Q. Yu, X.Y. Li, Extracellular polymeric substances (EPS) of microbial aggregates in biological wastewater treatment systems: a review, Biotechnol. Adv., 28 (2010) 882.
[11] E. Neyens, J. Baeyens, R. Dewil, h.B. De, Advanced sludge treatment affects extracellular polymeric substances to

improve activated sludge dewatering, J. Hazard. Mater., 106 (2004) 83–92.
[12] D. Xin, X. Chai, W. Zhao, Hybrid cement-assisted dewatering, solidification and stabilization of sewage sludge with high organic content. J. Mater. Cycles Waste Manage., 18 (2016) 356–365.
[13] L. Yu, Y. Yu, W. Jiang , H. Wei, C. Sun, Integrated treatment of municipal sewage sludge by deep dewatering and anaerobic fermentation for biohydrogen production. Environ. Sci. Pollut. Res., 22 (2015) 2599–2609.
[14] C.Y. Chen, P.Y. Zhang, G.M. Zeng, J.H. Deng, Y. Zhou, H.F. Lu, Sewage sludge conditioning with coal fly ash modified by sulfuric acid, Chem. Eng. J., 158 (2010) 616–622.
[15] V.K. Gupta, M. Gupta, S. Sharma, Process development for the removal of lead and chromium from aqueous solutions using red mud--an aluminium industry waste, Water Res., 35 (2001) 1125–1134.
[16] P. Kounalakis, K. Aravossis, C. Karayianni, Feasibility study for an innovative industrial red mud utilisation method, Waste Manage. Res., 34 (2016) 171.
[17] J. Yang, B. Xiao, Development of unsintered construction materials from red mud wastes produced in the sintering alumina process, Constr. Build. Mater., 22 (2008) 2299–2307.
[18] W. Liu, X. Chen, W. Li, Y. Yu, K. Yan, Environmental assessment, management and utilization of red mud in China, J. Clean. Prod., 84 (2014) 606–610.
[19] H. Gu, N. Wang, S. Liu, Radiological restrictions of using red mud as building material additive, Waste Manage. Res., 30 (2012) 961.
[20] Y.J. Liu, R. Naidu, M. Hui, Red mud as an amendment for pollutants in solid and liquid phases, Geoderma., 163 (2011) 1–12.
[21] S. Agatzini-Leonardou, P. Oustadakis, P.E. Tsakiridis, C. Markopoulos, Titanium leaching from red mud by diluted sulfuric acid at atmospheric pressure, J. Hazard. Mater., 157 (2008) 579–586.
[22] H. Zhang, J. Yang, W. Yu, S. Luo, L. Peng, X. Shen, Y. Shi, S. Zhang, J. Song, N. Ye, Mechanism of red mud combined with Fenton's reagent in sewage sludge conditioning, Water Res., 59 (2014) 239–247.
[23] P.E. Tsakiridis, G.D. Papadimitriou, S. Tsivilis, C. Koroneos, Utilization of steel slag for portland cement clinker production. J. Hazard. Mater., 152 (2008) 805–11.
[24] A. Altun, I. Yılmaz, Study on steel furnace slags with high MgO as additive in Portland cement, Cem. Concr. Res., 32 (2002) 1247–1249.
[25] H. Motz, J. Geiseler, Products of steel slags an opportunity to save natural resources, Waste Manage., 21 (2001) 285–293.
[26] D. Li, X. Fu, X. Wu, M. Tang, Durability study of steel slag cement. Cem. Concr. Res., 27 (1997) 983–987.
[27] M. Tuefekci, A. Demirbas, Evaluation of steel furnace slags as cement additives, Cem. Concr. Res., 27 (1997) 1713–1717.
[28] G. Qian, D.D. Sun, J.H. Tay, Z. Lai, G. Xu, Autoclave properties of kirschsteinite-based steel slag. Cem. Concr. Res., 32 (2002) 1377–1382.
[29] A. Monshi, M.K. Asgarani, Producing Portland cement from iron and steel slags and limestone, Cem. Concr. Res., 29 (1999) 1373–1377.
[30] J. Vaxelaire, J. Olivier, Conditioning for Municipal Sludge Dewatering. From Filtration Compression Cell Tests to Belt Press, Dry. Technol., 24 (2006) 1225–1233.
[31] M. Raynaud, J. Vaxelaire, P. Heritier, J.C. Baudez, Activated sludge dewatering in a filtration compression cell: deviations in comparison to the classical theory, Asia-Pac. J. Chem. Eng., 5 (2010) 785–790.
[32] B. Frølund, T. Griebe, P.H. Nielsen, Enzymatic activity in the activated-sludge floc matrix, Appl. Microbiol. Biotechnol., 43 (1995) 755.
[33] T.L. Poxon, J.L. Darby, Extracellular polyanions in digested sludge: Measurement and relationship to sludge dewaterability, Water Res., 31 (1997) 749–758.
[34] Y. Qiang, H.Y. Lei, G.W. Yu, F. Xin, Z.X. Li, Z.C. Wu, Influence of microwave irradiation on sludge dewaterability, Chem. Eng. J., 155 (2009) 88–93.
[35] X.Y. Li, S.F. Yang, Influence of loosely bound extracellular polymeric substances (EPS) on the flocculation, sedimentation and dewaterability of activated sludge, Water Res., 41 (2007) 1022–1030.
[36] Z. Xu, W. Qilin, J. Guangming, L. Peng, Y. Zhiguo, A novel conditioning process for enhancing dewaterability of waste activated sludge by combination of zero-valent iron and persulfate, Bioresour. Technol., 185 (2015) 416.
[37] G.P. Sheng, H.Q. Yu, Characterization of extracellular polymeric substances of aerobic and anaerobic sludge using three-dimensional excitation and emission matrix fluorescence spectroscopy, Water Res., 40 (2006) 1233.
[38] V. Urbain, J.C. Block, J. Manem, Bioflocculation in activated sludge: an analytic approach, Water Res., 27 (2011) 829–838.
[39] W. Zhang, P. Xiao, Y. Liu, S. Xu, F. Xiao, D. Wang, C.W.K. Chow, Understanding the impact of chemical conditioning with inorganic polymer flocculants on soluble extracellular polymeric substances in relation to the sludge dewaterability, Sep. Purif. Technol., 132 (2014) 430–437.
[40] M. Niu, W. Zhang, D. Wang, Y. Chen, R. Chen, Correlation of physicochemical properties and sludge dewaterability under chemical conditioning using inorganic coagulants, Bioresour. Technol., 144 (2013) 337.
[41] G. Zhen, X. Lu, Y. Zhao, X. Chai, D. Niu, Enhanced dewaterability of sewage sludge in the presence of Fe(II)-activated persulfate oxidation, Bioresour. Technol., 116 (2012) 259.
[42] T. Liu, Z.L. Chen, W.Z. Yu, S.J. You, Characterization of organic membrane foulants in a submerged membrane bioreactor with pre-ozonation using three-dimensional excitation-emission matrix fluorescence spectroscopy, Water Res., 45 (2011) 2111–2121.
[43] R. Artinger, G. Buckau, S. Geyer, P. Fritz, M. Wolf, J.I. Kim, Characterization of groundwater humic substances: influence of sedimentary organic carbon, Appl. Geochem., 15 (2000) 97–116.
[44] Z.W. Wang, Z.C. Wu, S.J. Tang, Characterization of dissolved organic matter in a submerged membrane bioreactor by using three-dimensional excitation and emission matrix fluorescence spectroscopy, Water Res., 43 (2009) 1533–1540.
[45] G. Zhen, X. Lu, Y. Li, Y. Zhao, B. Wang, Y. Song, X. Chai, D. Niu, X. Cao, Novel insights into enhanced dewaterability of waste activated sludge by Fe(II)-activated persulfate oxidation, Bioresour. Technol., 119 (2012) 7.
[46] P.G. Coble, Characterization of marine and terrestrial DOM in seawater using excitation-emission matrix spectroscopy, Mar. Chem., 51 (1996) 325–346.